

Comparing Feature Engineering and End-to-End Deep Learning for Autism Spectrum Disorder Assessment based on Fullbody-Tracking

Alberto Altozano Maria Eleonora Minissi Mariano Alcañiz Javier Marín-Morales

University Research Institute of Human-Centered Technologies
Universitat Politècnica de València (UPV)

{aaltfer,meminiss,malcaniz,jamarmo}@htech.upv.es

Abstract

*Autism Spectrum Disorder (ASD) is characterized by challenges in social communication and restricted patterns, with motor abnormalities gaining traction for early detection. However, kinematic analysis in ASD is limited, often lacking robust validation and relying on hand-crafted features for single tasks, leading to inconsistencies across studies. Thus, end-to-end models have become promising methods to overcome the need for feature engineering. Our aim is to assess both approaches across various kinematic tasks to measure the efficacy of commonly used features in ASD assessment, while comparing them to end-to-end models. Specifically, we developed a virtual reality environment with multiple motor tasks and trained models using both classification approaches. We prioritized a reliable validation framework with repeated cross-validation. Our comparative analysis revealed that hand-crafted features outperformed our deep learning approach in specific tasks, achieving a state-of-the-art area under the curve (AUC) of 0.90 ± 0.06 . Conversely, end-to-end models provided more consistent results with less variability across all VR tasks, demonstrating domain generalization and reliability, with a maximum task AUC of 0.89 ± 0.06 . These findings show that end-to-end models enable less variable and context-independent ASD assessments without requiring domain knowledge or task specificity. However, they also recognize the effectiveness of hand-crafted features in specific task scenarios.*¹

1. Introduction

Autism Spectrum Disorder (ASD) is a complex neurodevelopmental condition marked by social communication difficulties and restricted, repetitive patterns of behaviors and interests[1]. Detecting ASD at an early age is vital for initi-

ating timely interventions that can significantly enhance the quality of life for affected children [2]. However, current diagnostic methods rely heavily on subjective assessments, highlighting the pressing need for more objective, quantifiable means of detection.

Recently, motor abnormalities have surfaced as promising early biomarkers for ASD [3]. These abnormalities encompass a wide range of characteristics, from gross motor impairments affecting whole-body coordination and postural control to fine motor deficits affecting dexterity, handwriting, and object manipulation [4–13]. Additionally, stereotypical motor movements (SMMs) have also garnered significant attention for early diagnosis. SMMs refer to repetitive motions such as hand-flapping, finger-flicking, body rocking, body spinning, or head banging, that occur without a clear purpose or goal [14], with approximately 44% of patients reporting some form of SMM [15]. Remarkably, these movements tend to emerge before the age of 3, with around 80% of cases displaying repetitive movements by the age of 2 [16]. While the appearance rate of this symptom may not be exceptionally high, it underscores the potential for quantitatively studying the motor qualities of the ASD population, in conjunction with other motor abnormalities, as a means of understanding and diagnosing ASD in young population.

Recent advancements in technology, particularly motion sensors and computer vision algorithms, have enabled the automated assessment of motor characteristics in children with ASD. This progress has opened up new possibilities for more objective, data-driven ASD assessment, aiming to reduce reliance on expert judgments and enhance the accuracy and precision of early diagnosis.

Currently, ASD assessment methods that use kinematic data often hinge on hand-crafted features meticulously designed by domain experts, with only two articles using end-to-end models [17]. These features form the foundation for training machine learning models to distinguish between individuals with and without ASD. However, the creation and refinement of algorithms for feature extraction is a labor-intensive process, demanding careful parameter tuning, in-

¹This work has been submitted to the IEEE for possible publication. Copyright may be transferred without notice, after which this version may no longer be accessible

cluding considerations such as smoothing parameters, time window selection, or methodological considerations, which can significantly impact the results.

In contrast, certain research domains have shifted away from hand-crafted features in favor of alternative approaches that do not require specialized expertise or extensive engineering. Specifically, deep learning models that operate end-to-end have gained traction as comprehensive solutions, offering superior performance over traditional techniques in various domains, action recognition being one noteworthy example [18], which is also related to a movement classification task. However, adopting deep learning for ASD assessment brings its own set of challenges, particularly related to interpretability. Despite their potential to enhance ASD assessment and machine learning model development, the question remains whether these deep learning models can outperform meticulously crafted features in the context of early ASD diagnosis.

Another critical aspect of the current literature on ASD motor movement analysis is the limited validation of data models [13]. Amassing a large sample, particularly within the ASD population, poses significant challenges, resulting in studies often working with limited sample sizes. This limitation subsequently affects the size of the testing partition, with some studies forgoing one altogether due to constraints imposed by the size of the training sample. Nevertheless, a robust validation of machine learning models, especially when dealing with health-related data, necessitates the presence of a suitably sized unseen testing partition.

Considering these aforementioned challenges, the existing literature is subject to certain limitations. Firstly, hand-crafted metrics, although developed by experts, require generating hypotheses for feature selection using human knowledge [19], potentially leading to the unintentional omission of details or the neglect of alternative metrics that could improve the accuracy of ASD classification. Additionally, across diverse experiments or methodologies, even minor variations in data yield significant variability in hand-crafted feature selection [20], making it uncertain whether they can be applied more broadly. On the other hand, using end-to-end deep learning offers a chance to create models for evaluating various methodologies by automatically generating features [21], but it comes with challenges related to explaining how the model works. Therefore, it would be beneficial for the literature to conduct a thorough performance comparison, examining results across different scenarios and assessing the trade-off between generalizability and performance. Secondly, many studies could benefit from more extensive validation procedures to predict how well a model will perform on new data accurately.

To overcome these limitations, we propose two primary strategies. Firstly, we aim to develop multiple classification models based on the body movements of children engaged

in various motor tasks within a virtual reality (VR) environment. These models will utilize expert-defined metrics that have been previously employed in the literature [12, 13, 22–25]. We will compare these models with a novel, fully automated model designed for ASD classification. This approach entails the use of an end-to-end deep learning model capable of automatically detecting ASD without the need for manually defined metrics. This automated approach eliminates the need for metric engineering, allowing the model to autonomously extract its own features. Similar to the hand-crafted models, we will train one end-to-end model for each VR task, enabling us to perform a comparative analysis of model performance across different scenarios.

Secondly, to ensure a fair comparison and establish the validity of the trained models, we have implemented a robust validation strategy. Our strategy involves nested subject-dependent repeated cross-validation, utilizing a dataset comprising 81 subjects (39 with ASD and 42 typically developing). Our objective with this strategy is to ensure consistent and dependable performance that effectively generalizes to real-world, unseen data.

In summary, the main contributions of the work are (1) introducing a newly trained 3DCNN ResNet tailored for end-to-end kinematic ASD classification, using an existing deep learning architecture for action recognition; (2) demonstrating superior performance of both individual machine learning models and the end-to-end model compared to the State of the Art; (3) emphasizing model reliability through a dedicated focus on repeated cross-validation techniques, ensuring a reliable and accurate performance estimation; and (4) showcasing the end-to-end model’s capacity for enhanced generalization across various specific domain datasets.

2. Related Work

In the realm of ASD assessment through motion analysis, various research endeavors have enriched our understanding of the field. This section provides an overview of previous studies with a particular focus on hand-crafted features, robust validation methods, the utilization of multiple tasks for classification, and the application of deep learning models.

Several studies have employed hand-crafted features to characterize motion patterns associated with ASD. For example, Crippa *et al.* [12] employed metrics such as total movement, peak velocity, acceleration, and deceleration in their analysis. Simeo *et al.* [26] used features such as average speed, average maximum and minimum speed, and acceleration, while Zhao *et al.* [25] incorporated parameters like amplitude, entropy, mean, and maximum values of velocity and acceleration. It is crucial to note that these studies often grapple with limitations in their validation procedures. For instance, Crippa *et al.* [12] selected the feature set with the best testing performance, potentially introducing bias into their results. Simeo *et al.* [26] cross-validation method may

not be subject-dependent, which could affect the model’s generalizability. Similarly, Zhao *et al.* [25] explored every feature combination and reported the one with the best results, raising concerns about overfitting. These studies underscore the challenges in achieving unbiased validation in ASD assessment models.

In contrast, Vabalas *et al.* [13] prioritized robust validation processes to enhance result reliability. Their approach involved nested cross-validation along with a validation group, ensuring a more rigorous assessment of model performance. By testing the model on unseen data, they mitigated concerns of overfitting. Their model, utilizing support vector machines (SVMs) and feature selection, achieved a 73% accuracy. Vabalas *et al.*’ study exemplifies a commitment to dependable validation in the realm of ASD classification.

Alcañiz *et al.* [23] pursued a distinctive approach by exploring the use of multiple VR tasks for ASD classification. Their innovative experimentation involved 24 ASD and 25 typically developing (TD) participants aged 4 to 7. Metrics related to the total body movement range of various body parts were extracted and used to train a SVM with recursive feature elimination (RFE). This approach resulted in an 80.29% accuracy. Notably, their study leveraged the potential of employing a diverse set of tasks to enhance ASD assessment through motion analysis while being able to test a model on multiple scenarios in order to compare task performance and model generalizability.

deep learning models have also made a significant impact on motion-based ASD classification. Zunino *et al.* [27] harnessed the power of a convolutional neural network (CNN) coupled with a long short-term memory (LSTM) network to analyze short raw videos of subjects engaged in reach and grab tasks. This innovative approach achieved a 75% accuracy, showcasing the feasibility of deep learning techniques in motion analysis for ASD assessment. In a parallel effort, Kojovic *et al.* [28] conducted an expansive study involving 169 subjects, a majority of whom had ASD. They employed deep learning techniques, including skeleton-based body tracking, and achieved an impressive 82.98% accuracy. This study underscored the potential of deep learning in deciphering complex motion patterns linked to ASD.

In our study, we have synthesized key elements from these preceding works. We incorporated hand-crafted features akin to those employed by Zhao *et al.*[25], Simeo *et al.* [26], and Crippa *et al.*[12] for characterizing motion. Furthermore, we adopted the strategy of Alcañiz *et al.* [23] by using multiple VR tasks to train models based on these hand-crafted features. Additionally, we explored the potential of end-to-end deep learning models, as demonstrated by Zunino *et al.* [27] and Kojovic *et al.* [28]. Our primary objective is to comprehensively assess the performance of these approaches, highlighting their performance and generalization advantages and challenges in the context of early

ASD assessment. Notably, our study places a strong emphasis on robust validation, utilizing subject-dependent repeated cross-validation in every task model to ensure the reliability of our results and generalizability of our findings across different scenarios and tasks.

3. Materials

In our research, we adopted a VR approach to assess ASD and TD individuals from multiple virtual tasks, drawing inspiration from the work of Alcañiz *et al.* [23]. The utilization of VR aimed to create a sense of presence, fostering realistic responses and facilitating the collection of organic and ecological data. This approach offers several advantages for ASD assessment as it allows researchers to immerse subjects in controlled environments with social and motor interactive scenarios, directly relevant to ASD research, while maintaining a high degree of scalability and standardization.

3.1. Participants

In total, 81 children (42 with TD and 39 with ASD) took part in the study. Participants’ ages ranged between 3 and 7 years. The group of children with ASD was composed of 32 males and 7 females, and their mean age in months was 53.14 (SD = 12.38). The group of children with TD gathered 19 males and 23 females with a mean age in months of 57.88 (SD = 11.62). The sex imbalance between groups was in line with the prevalence ratio of the disorder (4 males, every 1 female diagnosed [29]). Children in the ASD group had a previous ASD diagnosis made by the administration of the Autism Diagnostic Observation Schedule-2 (ADOS-2; Lord *et al.* [30]). On the contrary, the absence of either diagnosis or risk of clinical disorders was required to be included in the TD group. Participants of both groups were Spanish and right-handed. They were drug naïve and had normal or corrected to normal vision. It should be noted that all participants’ caregivers signed a consent agreement form before the virtual experience took place.

3.2. The Experimental Setup and data collection

Due to concerns regarding discomfort in ASD individuals while using traditional head-mounted displays (HMDs) [31], we opted for the CAVE Automatic Virtual Environment (CAVE) as our VR system [32–34]. Unlike traditional HMDs, this setup eliminates problems related to cybersickness and the discomfort caused by ill-fitting HMDs, which can be challenging for individuals with ASD, especially young children. The CAVE room (4 m x 4 m x 3 m) is equipped with three ultra-short lens projectors positioned in the ceiling, projecting wide 100° images at a distance of 55 centimeters. The main components of the virtual scenes were displayed on the central (3 m x 4 m) wall, while the projections on the two (4 m x 4 m) lateral surfaces enhanced the participants’ sense of being within the virtual environment.

Task Name	Abbreviature	Block	Description/Task Objective
VE Presentation	PEAP	-	Both virtual avatars introduce themselves and familiarize the participant with the virtual environment. The participant is expected to remain still.
Introduction	I2	-	The principal avatar asks three questions to the participant regarding their well-being, favorite game, and preferred means of transportation, which the participant is required to verbally answer. If needed, pictograms appear to pick a response by pointing at it.
Bubble Task	T2A1	A	Participants must interact with the virtual environment by touching and blowing up 30 descending bubbles, each with different speed levels.
Apple Task	T2A2	A	Participants are tasked with grabbing an apple hanging from a virtual tree and placing it on the floor, repeating this action five times (top to bottom movement).
Kick Task	T2A3	A	The principal avatar passes a ball to the participant, who is invited to kick the ball three consecutive times.
Flower Task	T2A4	A	Participants must pick a virtual flower nearby and place it on a bench, repeating this action five times (left to right movement).
Hide & Seek Task	T2A5	A	The principal avatar hides in the virtual park, and the participant must indicate the avatar’s hiding spot by pointing at it. This is repeated three times with different hiding spots.
Step Task	T2B1	B	Participants are asked to imitate a sideways step movement demonstrated by the principal avatar, repeating this action five times.
Posture Task	T2B2	B	Participants are asked to imitate a specific posture demonstrated by the principal avatar, repeating this action five times.
Highfive Task	T2B3	B	Participants are required to virtually highfive the principal avatar five times.
Greeting Task	T2B4	B	Participants are required to greet the principal avatar five times using virtual interaction.
Final Scene	EF	A/B	The principal avatar concludes the virtual experience by asking the participant about their favorite game in the virtual environment. If needed, pictograms appear to pick a response by pointing at it.

Table 1. Description of the proposed VR tasks.

To enable participants’ interactions within the virtual environment, we employed an Azure Kinect DK, equipped with an RGB-D camera capable of capturing at 30 frames per second. The camera, in conjunction with a real-time computer vision algorithm, tracked 32 different body joints representing the user’s body position. As a result, we were able to create a dynamic silhouette of the participant, mirroring their movements into the virtual environment.

Additionally, the data obtained from the Azure Kinect DK was stored in a text file. Each line in the file contained: the 3D position of each joint at a specific frame, a corresponding timestamp, and a unique identifier for each body detected in the scene by the computer vision algorithm.

3.3. The Virtual Experience

The virtual environment, developed using Unity, simulated a playpark within an urban setting. It featured two virtual avatars: a child-like principal avatar, fostering social interaction and offering guidance on a series of engaging games

and tasks, and a virtual therapist avatar, an adult figure that stepped in to assist participants whenever their interactions deviated from the expected behavior. The therapist avatar was a source of reassurance, providing helpful explanations to aid participants in completing the tasks.

In Table 1, we present the 12 tasks included in the virtual experience, along with their abbreviations, block assignments, and objectives. Specifically, block A refers to tasks that involve interacting with the virtual environment, while block B focuses on gesture imitation. Participants were given 45 seconds to make progress in each task objective, with three consecutive failures leading to task termination and to the initialization of the next task.

To ensure that every participant had a diverse and unbiased experience, the order of blocks and tasks within each block was randomized. However, the presentation and introduction always occurred at the beginning of the experience, while the final scene was reserved for the end, regardless of the block order.

4. Methods

4.1. Data Preprocessing

Initially, the Azure Kinect DK provided the joint positions of the detected bodies in its field of view using a computer vision algorithm in a text log. However, upon initial inspection, it was found that the text log of joint positions included not only the participants tracked body, but also, in some cases, additional bodies were recognized by the sensor that were present in its field of view, such as the supervising researchers, who were present in the scene. Additionally, sampling rate was not uniform and there were missing values, which could lead to anomalies in engineered features (as it would be the case of instant velocity) or an uneven framerate in the case of generating videos from the tracking data.

To address these issues, we employed two strategies. First, participants were identified throughout the experience using a time-windowed function over time that saved the most repeated tracked body in a time window every step it is applied. Simultaneously, we monitored the centroid of the tracked body to ensure continuous movement. Specifically, to classify a user as valid, two criteria needed to be met: firstly, the centroid of the tracked body had to exhibit continuous movement, defined as a displacement of less than 30cm between frames. Secondly, the user selected should be the most frequently tracked body within 10-second windows. This approach allowed us to extract tracking data exclusively for the participants in the experiment, provided that they were the most commonly tracked bodies and displayed relatively smooth movement, as per our two primary assumptions. This cleaning process was validated visually for all users, and it proved to eliminate all tracked body duplicated from the original data. Then, a forced sampling rate of 10Hz was applied to all Azure Kinect DK text files by interpolating the data and eliminating the rest of the datapoints in order to solve the uneven framerate. This method also solved the appearance of missing values, which were interpolated throughout the scene using the position of each joint before and after the missing value.

4.2. Hand-crafted features approach

4.2.1 Data processing for feature engineering and machine learning

In order to obtain the hand-crafted features inspired by previous literature [12, 13, 22–25], such as velocity, position, or acceleration, we implemented a set of mathematical functions. These functions included the computation of the Euclidean distance between joints in consecutive frames, the calculation of derivatives for the time series of each joint, and the determination of the magnitude of vectors based on the three spatial coordinates.

Using these mathematical functions, we obtained time series data for various physical parameters, including displacement, velocity, acceleration, and tangential acceleration. Subsequently, we extracted relevant features from these time series. Specifically, we computed key statistical descriptors: the mean, variance, maximum, and minimum values, for the time series data of each joint.

However, this approach resulted in a substantial number of kinematic features that exhibited high correlation with each other due to joint proximity. To address this issue, we performed an aggregation step, wherein neighboring joint features were combined into larger body parts. This aggregation was achieved by computing the mean of the corresponding features for each independent body group. The defined body part groups included head, body and left and right arms, legs, feet, and hands, respectively. For a visual representation of these body part groups, refer to Figure 1.

4.2.2 Feature engineered machine learning models

Once the hand-crafted features were generated for every subject and task, initial assessment was explored using one of the training partitions. As a result, it was noted that non-linear machine learning models, such as rbf-SVM or kPCA with classifiers, consistently exhibited inferior performance compared to simpler linear algorithms. Therefore, in order to establish a meaningful comparison with existing literature, which predominantly employ linear models, we employed a LinearSVM with Recursive Feature Elimination with Cross-Validation (RFECV) as a wrapper, in addition to a Random Forest Classifier.

Our model fine-tuning aimed to maximize the Receiver Operating Characteristic - Area Under the Curve (ROC-AUC), albeit through slightly distinct approaches. Specifically, for the LinearSVM with RFECV, we executed a three-tiered nested cross-validation process, delineated as follows:

1. Feature Selection using RFECV: This entailed the selection of the optimal number of features through stratified k-fold cross-validation, with five folds considered for each C regularization parameter, ranging from 2^{-6} to 2^7 .
2. Hyperparameter Optimization: Subsequently, having determined the optimal number of features for every C regularization parameter, the most suitable C value was selected. This phase entailed another level of repeated stratified k-fold cross-validation, comprising 5 folds and 6 repetitions, and was conducted on the entire training partition. This step was executed subsequent to the feature selection phase.
3. Model Assessment: The third and outermost layer of cross-validation was reserved for assessing the overall model performance, as elucidated in Subsection 4.5, under our chosen validation strategy.

In essence, our approach for fine-tuning the LinearSVM

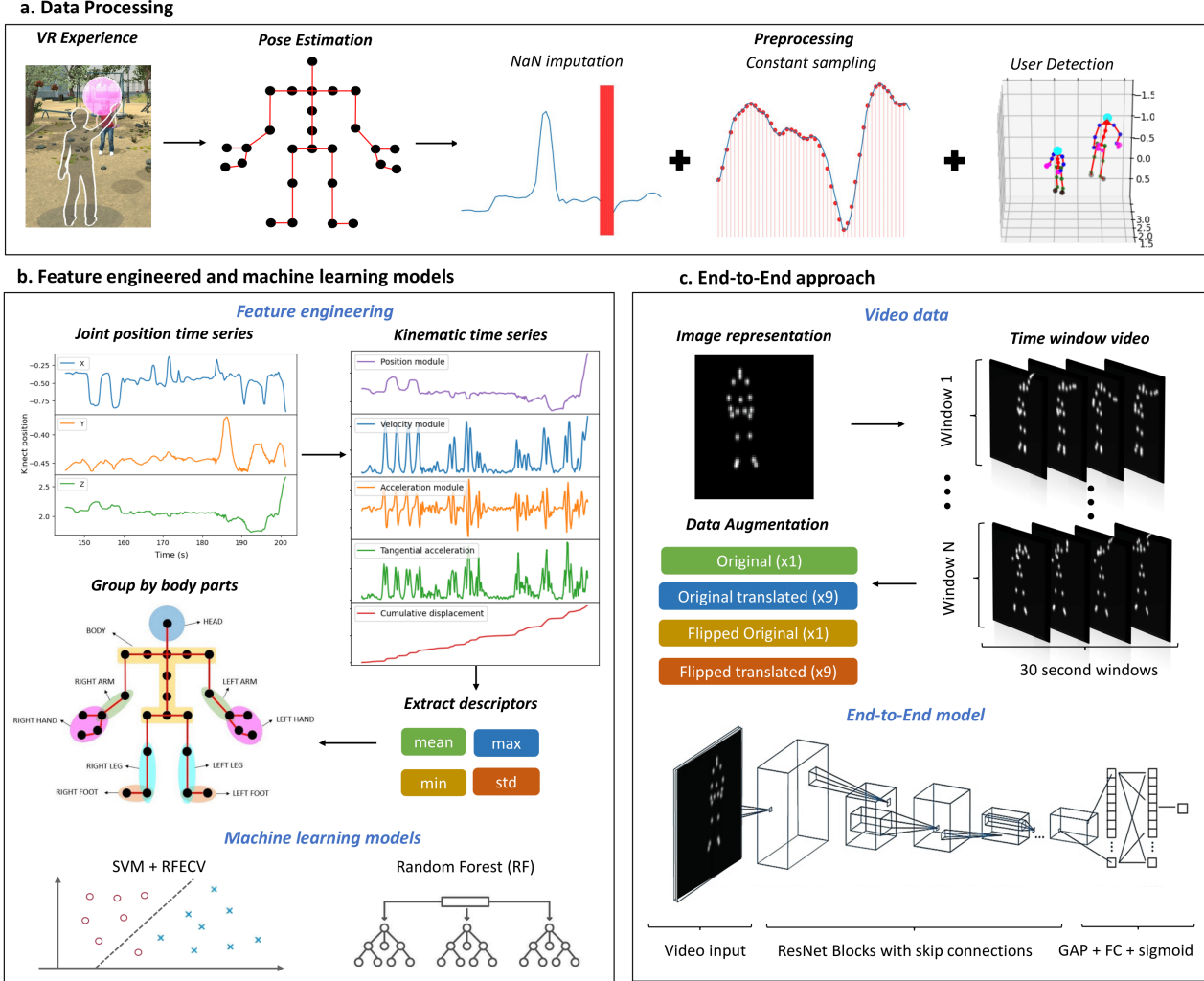


Figure 1. Visual representation of the proposed methodology. Top box represents the processing pipeline, from raw data to the data used for both the feature engineering and end-to-end approaches. Bottom left box represents the feature extraction process and the machine learning models used. Bottom right box represents the video generation process from raw data, the data augmentation process and our proposed end-to-end model.

with RFECV involved a rigorous three-level nested cross-validation process, wherein the first level focused on feature selection, the second on regularization parameter selection, and the third on model performance assessment.

In contrast, the fine-tuning of the Random Forest Classifier followed a simpler approach. In this case, our grid search efforts concentrated on optimizing the tree depth hyperparameter, spanning the range of $\text{maxdepth} \in [1, 2, 3, 4, 5, 6]$. Consequently, we engaged in a conventional two-tiered cross-validation process. The initial level, identical to the second level of the LinearSVM, addressed regularization hyperparameter selection, while the subsequent outer level was utilized for model performance evaluation.

4.3. End-to-end approach

4.3.1 Data processing for end-to-end deep learning

To prepare the input data for our deep learning model, we transformed the preprocessed joint time series into videos, representing them as sequences of pixel intensities. This conversion involved associating each time sample from all joints with an image, effectively generating individual frames that visually represent limb positions. Importantly, the framerate of these videos matched the input's preprocessed joint time series, which was set at 10Hz. This process resulted in video sequences with a resolution of 78 x 64 pixels for each subject and virtual task, an example of which is presented in Figure 1.

To portray body tracking joints in a 2D context, we adopted an algorithm inspired by Haodong *et al.*' [35] approach. Initially, we mapped each pixel in a frame into the Kinect's coordinate system. This mapping was achieved by interpolating distances across a regular grid that spanned between the maximum and minimum x_j and y_j positions of each joint. Equations 1 and 2 describe this pixel-to-coordinate transformation, where x_p and y_p represent the horizontal and vertical pixel coordinates in the Kinect's space, respectively. Additionally, h and v denote the pixel numbering along the frame's horizontal and vertical axes, while H and V signify the total number of pixels in the frame, horizontally and vertically.

$$x_p(h) = \min(x_j) + \frac{h}{H} (\max(x_j) - \min(x_j)) \quad (1)$$

$$y_p(v) = \min(y_j) + \frac{v}{V} (\max(y_j) - \min(y_j)) \quad (2)$$

Subsequently, pixel intensities for each frame were calculated based on the proximity of each pixel to the joints. Specifically, we employed the x and y components of the joints as the means for 2D normal distributions. The pixel intensity was then computed as the cumulative probability of a pixel being sampled from these Gaussian distributions, as outlined in Equation 3. Here, $I(x_p(h), y_p(v))$ represents the pixel intensity at position h, v , σ denotes the standard deviation parameter for the normal distribution, and x_j and y_j indicate the positional components of each joint. Importantly, this representation heightened the intensities of pixels closer to the joints, effectively highlighting the joints positions in the frame, while background pixels received intensities close to zero.

$$I(x_p(h), y_p(v)) = \sum_{j \in \text{Joints}} \frac{1}{\sigma\sqrt{2\pi}} e^{-\frac{1}{2} \left(\frac{(x_p, y_p) - (x_j, y_j)}{\sigma} \right)^2} \quad (3)$$

4.3.2 Data augmentation for Deep Learning

During the video generation process, it became apparent that participants were not in identical horizontal starting positions, leading to minor horizontal discrepancies across subjects. These discrepancies had the potential to divert the model's focus towards distinguishing subjects based on position rather than capturing general movement characteristics. Additionally, due to the intricate nature of deep learning models, a substantial volume of examples is required for effective generalization.

To address these concerns and enhance model generalization, we employed data augmentation techniques. Specifically, for every video and user, we generated an additional set

of 10 videos in both training and testing partition. This generation involved introducing a random horizontal variation to all joint positions. The extent of variation was determined by adding a constant random value (ϵ), sampled from a normal distribution characterized by a mean (μ_x) of 0 and a standard deviation (σ_x) of 0.35. The choice of σ_x was deliberate, ensuring that approximately 99% of the samples fell within the range of $x_j \in [\min(x_j), \max(x_j)]$. Furthermore, we created another set of 10 videos by horizontally flipping each of the previously generated ones. This process resulted in a total of 20 videos derived from each original video sample, effectively augmenting the dataset size and introducing valuable variability.

4.3.3 End-to-end Deep Learning model

In our pursuit of ASD assessment using deep learning, we trained and implemented from scratch the PoseConv3D architecture, a tailored spatio-temporal residual 3DCNN model originally introduced by Haodong *et al.* [35] for action recognition tasks in 15-second body tracking videos. This architecture showcases potential for ASD detection through movement data, harnessing its capacity to capture spatial and temporal details within movement patterns. Drawing inspiration from Haodong *et al.*' work, our model operates on videos featuring body-tracked joints superimposed on a consistent background. This approach empowers the model to focus on pertinent body parts, effectively filtering out background noise and RGB video complexities. Moreover, the spatio-temporal nature of the network, with convolutions spanning both spatial and temporal dimensions, enables the identification of crucial motion patterns vital for classifying children's movements within the virtual environment.

In terms of architectural details, our proposed deep neural network closely follows the PoseConv3D SlowOnly model introduced by Haodong *et al.* [35] for action recognition tasks, maintaining consistent layer counts, pooling layers, and kernel sizes. However, we introduced a modification to the final activation layer to tailor it to our specific binary classification problem of differentiating between ASD and non-ASD cases. In contrast to Haodong *et al.*' original model, we employed a single-neuron sigmoid activation for this layer. Our modification of PoseConv3D architecture is illustrated in Table 2, where the dimensions of kernels are denoted by $T \times S^2, C$ for temporal, spatial and channel sizes and GAP denotes global average pooling. Moreover, certain hyperparameters were determined based on unique considerations specific to our study. Computational and memory constraints guided our choices for batch size and temporal sample size. Consequently, we selected a batch size of 3 and designed our subject samples to span 30 seconds. This decision ensured efficient memory utilization while accommodating the need for capturing a broader tem-

Stage	PoseConv3D (SlowOnly)	
Data Layer	Uniform : $T \times (78 \times 64), 1$	
Stem Layer	$[1 \times 7^2, 32] \times 1$	
Stage 1	$1 \times 1^2, 32$ $1 \times 3^2, 32$ $1 \times 1^2, 128$	$\times 4$
Stage 2	$3 \times 1^2, 64$ $1 \times 3^2, 64$ $1 \times 1^2, 256$	$\times 6$
Stage 3	$3 \times 1^2, 128$ $1 \times 3^2, 128$ $1 \times 1^2, 512$	$\times 3$
Output Stage	Global Average Pooling (GAP) Fully connected Layer (FC) Sigmoid activation	

Table 2. End-to-End ResNet 3DCNN architecture.

poral context in ASD assessment. Unlike action recognition tasks, which may rely on shorter video segments, ASD classification benefits from more extensive temporal information. This extension of video length from Haodong *et al.*' original 15 seconds to 30 seconds was essential for providing our model with the necessary context for accurate assessments. It's worth noting that the tasks within the virtual experience typically lasted 1 to 3 minutes, resulting in multiple videos for each user, each covering a 30-second interval with 15-second overlaps. Subsequently, the final prediction for each user was generated by aggregating the voting predictions derived from all these overlapping windowed videos.

Conversely, the establishment of suitable values for the number of epochs and the learning rate relied on initial exploratory experiments conducted using a single training set. Following this preliminary validation, it was determined that a training regimen comprising 200 epochs, each consisting of 100 minibatches, produced favorable outcomes without introducing the risk of overfitting. To optimize our model, we employed a cross-entropy loss function in conjunction with Stochastic Gradient Descent (SGD) with a learning rate set to 0.01. A *ReduceOnPlateau* strategy was applied, incorporating a patience parameter of 10 epochs, to dynamically adjust the learning rate as training progressed. Additionally, given the limited validation data and the potential susceptibility to overfitting, we implemented an early stopping mechanism with a patience setting of 25 epochs to provide an additional layer of protection against this risk.

4.4. Task-Specific and voting models

The virtual experience offers a range of diverse tasks, each designed to engage users differently. To thoroughly evaluate the efficacy of both deep learning and feature engineering approaches in ASD assessment, we constructed distinct models

tailored to each specific task within the virtual environment. This approach allowed us to create individual models for each task, enabling a thorough comparison between feature engineering techniques and the deep learning model in various contexts.

Furthermore, we introduced an ensemble method to consolidate predictions generated by these task-specific models. Instead of combining all predictions into one, we established three distinct ensemble models: one for the task-specific LinearSVM models, one for the task-specific Random Forest models, and one for the task-specific end-to-end model. For each ensemble model, the predictions from task-specific models are aggregated by calculating the mean of the predicted probabilities. By aggregating predictions from feature-engineered models within each task category and, similarly, for the end-to-end model, we can evaluate their collective performance in ASD assessment, enabling a more meaningful model comparison.

4.5. Validation Strategy

Our validation strategy for assessing model performance involves a subject-dependent repeated stratified k-fold approach with 4 folds and 2 repetitions, totaling 8 folds (refer to Figure 2). Specifically, we partition participants into stratified folds based on their respective groups, ensuring a proportional representation from each group within each fold. Following this division into training and testing partitions, we create task-specific datasets. For each of the 12 virtual tasks, we establish two datasets: one containing task-specific hand-crafted features and another with task-specific kinematic windowed videos, resulting in a total of 24 datasets.

Within each fold, we train all models, including feature-engineered and deep learning models, using the generated datasets. Deep learning models utilize the 12 video datasets, while machine learning models (Random Forest and LinearSVM) operate on the 12 feature-engineered datasets. Feature-engineered models undergo additional fine-tuning during training (see subsection 4.2.2), making our strategy a nested cross-validation. In contrast, end-to-end models use fixed hyperparameters and do not require fine-tuning. Following training, all models are tested on the corresponding 12 test datasets, which share the same subjects to ensure a fair model comparison. After training, we test all models on corresponding test datasets with the same subjects to ensure a fair comparison. We aggregate model predictions using a voting system to evaluate the performance of feature-engineered and end-to-end models across all tasks and their ensemble performance.

In order to validate each model's performance a set of metrics were considered: accuracy (i.e., percentage of subjects correctly recognized), true positive rate (i.e., percentage of ASD subjects correctly labelled), true negative rate (i.e.,

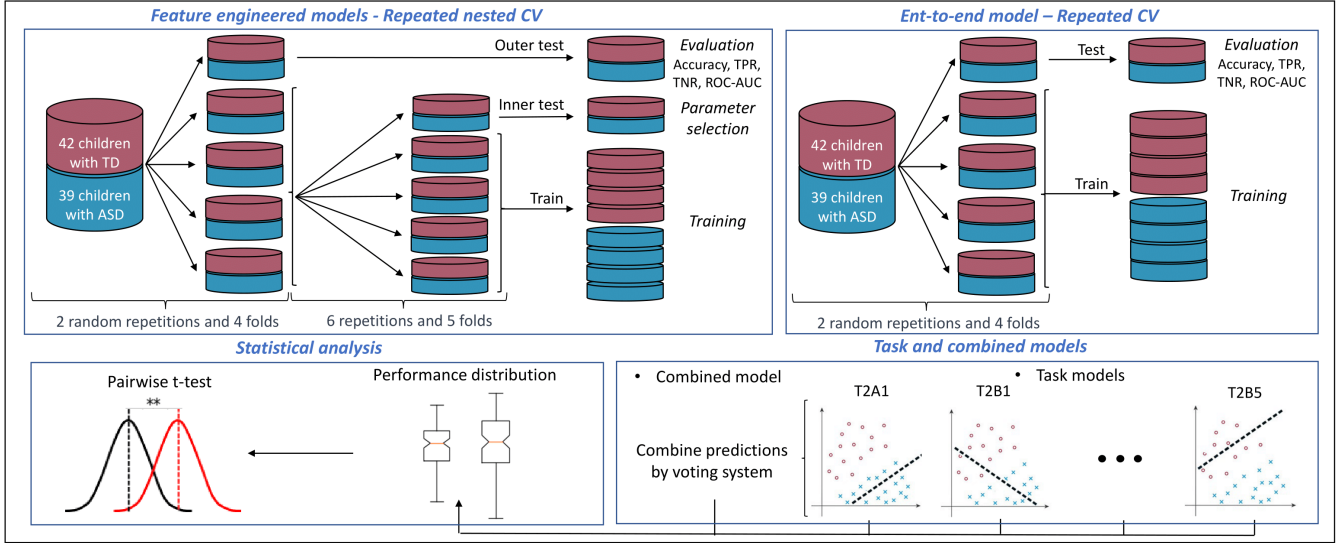


Figure 2. Representation of the validation strategy. Top boxes show our cross validation strategies for both the end-to-end and feature engineered models. Bottom right represents our voting system for the ensemble model, which combines task-specific model predictions. Bottom left depicts the pairwise statistical analysis used for model comparison.

percentage of control subjects recognized as control), and Receiver Operating Characteristic Area Under the Curve (ROC-AUC), which describes the model’s ability to differentiate between positive and negative classes, with a value of 0.5 indicating performance equivalent to random classification and a value of 1 signifying perfect discrimination.

5. Results

Table 3 presents the mean and variance of the test performance results across all folds and for each of the proposed models: the end-to-end models and the models trained with handcrafted features for each game, along with their ensemble global voting and the aggregated mean performance across all games. Variability was observed across games and k-fold splits, with some tasks yielding higher performance than others. Notably, tasks related to gross motor coordination (e.g., T2A1, T2A3, T2B1) achieved high accuracies of over 80% and ROC-AUC values of 0.85 to 0.90, denoting outstanding performance for binary classification.

Regarding the feature-engineered models (SVM+RFECV and Random Forest), they outperformed the end-to-end model in 7 out of 12 goal-oriented models in terms of accuracy. Specifically, the LinearSVM surpassed the deep learning approach in 6 out of 12 games, while the Random Forest surpassed it in 4 out of 12. Although the feature-engineered models generally showed slightly better accuracies, their largest improvement over deep learning was only 6% in the T2B3 task, with the rest showing smaller improvements. On the other hand, deep learning outperformed the feature-engineered models by up to 9% in T2A5, 7% in

PEAP, and 6% in T2A2. These differences are further evident in the mean accuracies across games, favoring the deep learning model. It achieved a higher mean accuracy despite outperforming feature-engineered models in only 5 out of 12 tasks. However, when deep learning did outperform the feature-engineered models, it did so more significantly than when the feature-engineered models outperformed the deep learning model.

Regarding ROC-AUC, the end-to-end deep learning model showcased consistently higher results, outperforming feature-engineered models in 9 out of 12 games. The LinearSVM+RFECV surpassed the ROC-AUC in 1 game, while Random Forest did so in 2. The end-to-end model showed significant improvements in ROC-AUC compared to feature-engineered models, with some cases showing over 0.10 improvements, particularly in PEAP, where it achieved a remarkable 0.18 increase. These results support the findings from the accuracy results, indicating that the end-to-end model significantly improved performance in games where feature-engineered models performed poorly.

Nevertheless, these differences in accuracy and ROC-AUC between end-to-end and feature-engineered models can be partially explained by the TPR and TNR metrics. Feature-engineered models consistently exhibited high TNR and lower TPR, while the end-to-end model achieved a more balanced TPR and TNR, resulting in higher ROC-AUC values. Although feature-engineered models achieved slightly higher accuracies more frequently, particularly due to the dataset’s slight negative class bias, the end-to-end model demonstrated better overall balance and consistency in distinguishing between classes.

Game	Model	Accuracy	TPR	TNR	AUC
EF	PoseConv3D	72±08	72±17	74±12	78±08
	SVM+RFECV	73±08	58±22	85±07	72±15
	Random Forest	72±08	57±28	84±14	75±17
I2	PoseConv3D	56±16	80±18	38±35	71±11
	SVM+RFECV	56±20	50±32	65±30	63±28
	Random Forest	57±16	53±19	60±24	52±18
PEAP	PoseConv3D	71±09	87±18	59±20	82±10
	SVM+RFECV	59±14	62±15	57±16	63±18
	Random Forest	64±14	64±19	64±15	64±16
T2A1	PoseConv3D	83±12	75±19	88±07	84±11
	SVM+RFECV	85±03	85±13	85±13	90±06
	Random Forest	84±07	81±12	86±08	87±10
T2A2	PoseConv3D	81±11	74±15	85±12	79±15
	SVM+RFECV	65±06	54±16	72±11	64±19
	Random Forest	75±12	50±20	90±13	77±14
T2A3	PoseConv3D	78±13	68±17	86±12	86±12
	SVM+RFECV	79±11	73±19	84±14	84±11
	Random Forest	81±12	75±21	86±09	86±14
T2A4	PoseConv3D	69±15	47±22	83±16	81±15
	SVM+RFECV	58±23	35±30	73±27	62±26
	Random Forest	66±18	50±28	77±18	69±24
T2A5	PoseConv3D	75±09	51±25	89±10	81±10
	SVM+RFECV	66±15	38±31	86±9	65±27
	Random Forest	64±14	35±33	80±11	71±21
T2B1	PoseConv3D	78±11	63±19	89±12	89±06
	SVM+RFECV	82±08	78±13	85±15	88±08
	Random Forest	76±09	61±23	86±12	85±09
T2B2	PoseConv3D	76±10	54±17	91±10	72±12
	SVM+RFECV	77±12	70±17	82±14	81±09
	Random Forest	74±11	61±16	83±13	82±08
T2B3	PoseConv3D	73±09	66±18	78±12	83±09
	SVM+RFECV	76±12	65±17	82±16	82±10
	Random Forest	79±11	55±15	96±08	76±09
T2B4	PoseConv3D	74±09	55±14	87±11	77±11
	SVM+RFECV	67±08	46±06	84±12	75±07
	Random Forest	69±07	46±16	87±09	78±06
Mean	PoseConv3D	74±03	66±03	79±07	80±03
	SVM+RFECV	70±06	60±08	78±07	74±08
	Random Forest	72±04	57±06	82±05	75±06
Global Voting	PoseConv3D	77±10	74±20	80±07	86±10
	SVM+RFECV	77±13	64±20	87±17	82±13
	Random Forest	80±11	68±19	90±10	83±16

Table 3. Outer test performance results for end-to-end and handcrafted feature models, ensemble voting, and mean performance aggregates

5.1. Model Comparison and Statistical Analysis

One of the primary objectives of this study was to conduct a comprehensive comparison between feature-engineered and end-to-end models across various application contexts, assessing their generalization capabilities in diverse kinematic tasks. Figure 3 represents the ROC curves of each model across all folds and tasks. The highlighted area for each model represents the standard deviation of the mean in each point of the curve. To facilitate model comparison across tasks, we aggregated the ROC-AUC results from all folds and tasks into performance distributions. Figure 4 provides a visual representation of the ROC-AUC scores for both feature-engineered models and the deep learning model across all aggregated folds and tasks.

Statistical analysis, including a T-test, was performed to compare all models, revealing no statistically significant differences in their mean ROC-AUC distributions ($p > 0.05$). However, the application of a Levene test indicated significant differences in variances among the AUC of the models. Instances marked with an asterisk (*) in Figure 4 signify statistical significance, highlighting situations where performance variance differences between models are significant. Figure 4 illustrates that while differences in performance are not highly pronounced, the end-to-end deep learning model exhibits lower model variance and a more stable distribution. This is also visually supported by Figure 3, where it can be appreciated that the standard deviation is lower for the end-to-end deep learning model throughout the ROC curve.

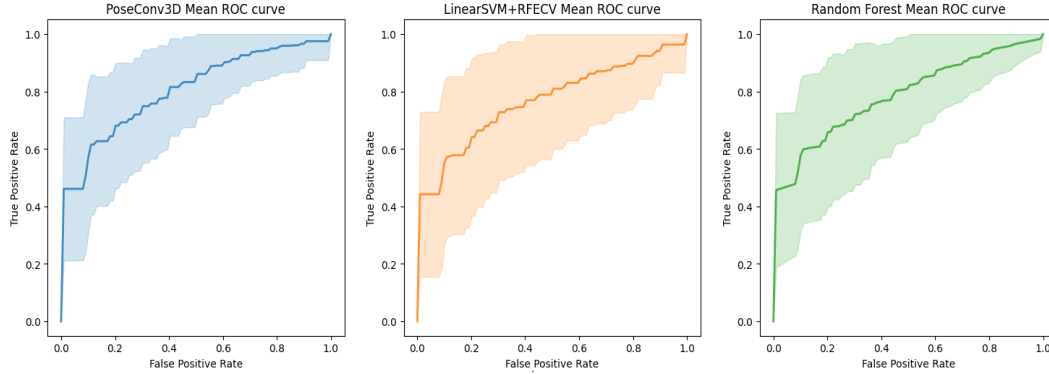


Figure 3. Mean ROC curves and standard deviations (highlighted) across models for all folds and games.

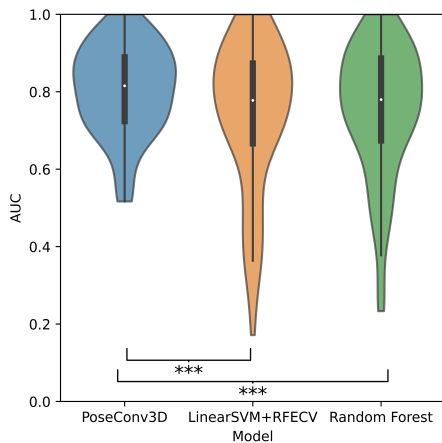


Figure 4. Levene performance differences across models.

6. Discussion

In this study, our primary objective is to compare the performance of end-to-end deep learning models with hand-crafted feature models across various scenarios. To achieve this objective, we recruited a total of eighty-one children aged between 3 and 7 years, segregating them into two groups: ASD, comprising children with a confirmed diagnosis of the disorder, and a control group. Participants engaged in a VR scenario, where they interacted with a virtual environment and completed diverse tasks. An RGB-D camera recorded their body movements during these tasks, serving as input for training an end-to-end deep learning model based on spatio-temporal kinetic data, as well as two models trained with hand-crafted features characterizing movement.

6.1. Model Performance and Statistical Differences

Our findings indicate that feature-engineered models generally exhibited higher accuracy than the end-to-end model across most tasks, such as tasks involving touching moving objects or action imitation. However, these improvements

were typically modest, ranging from 1% to 6%, with an average improvement of 2.6%. Conversely, there were instances where the end-to-end model outperformed the hand-crafted models, with accuracy improvements ranging from 3% to 7% and averaging 6%, leading to the end-to-end model achieving a superior mean accuracy across tasks. Another important outcome is that our end-to-end model showed a higher mean TPR than the feature-engineered models, with only a slight decrease in TNR. This resulted in a more balanced TPR-to-TNR ratio, enhancing class distinguishability, particularly evident in the ROC-AUC. On average, the end-to-end model outperformed the feature-engineered models in terms of ROC-AUC by 0.05. It should be noted the slight superiority of the end-to-end deep learning model was achieved even when placing the model at a comparative disadvantage, as the hand-crafted models underwent fine-tuning using an internal validation strategy for every fold, whereas the end-to-end model’s hyperparameters were selected using a single external validation.

However, we cannot definitively conclude that end-to-end deep learning models consistently outperform feature-engineered models across various tasks and contexts, as our t-test did not reveal significant differences in ROC-AUC mean distributions across all folds and tasks. This could be attributed to greater variability and uncertainty in task-specific performance compared to mean performance differences. Nevertheless, the Levene test indicated significant differences between distributions, suggesting that ROC-AUC exhibited less variability across tasks and folds for the end-to-end model ($p < 0.001$). This indicates that the end-to-end model is more stable and robust, consistently engineering features that better distinguish both classes across a broader range of contexts and tasks than hand-crafted features. These results emphasize the potential of end-to-end models to adapt across different application contexts. Specifically, results suggest that end-to-end models can effectively extract features even in cases where feature engineering falters, while the opposite isn’t as significant.

In summary, although there is no statistically significant evidence confirming that end-to-end models consistently outperform feature-engineered models, they do exhibit statistically higher reliability and consistency in their results across datasets obtained in different contexts in ASD assessment. Furthermore, end-to-end models are easier to implement, eliminating the need for defining hand-crafted metrics. However, machine learning models demonstrate higher accuracy in certain contexts, while offering advantages in terms of explainability and ease of training.

6.2. Comparison with State-Of-the-Art

In the realm of ASD assessment, few studies have explored full-body tracking. However, these studies often grapple with validation limitations [12, 25, 26]. To ensure the practical applicability of ASD assessment, it is paramount to accurately identify the disorder. Researchers should focus on subject-dependent cross-validations and meticulous separation of unseen test data. Examples of practices to be avoided include training models with various feature sets or hyperparameters sets and reporting the best result. These examples all fall under the umbrella of model selection strategies, which must be externally validated with real unseen test datasets to assess their effectiveness. This work distinguishes itself by emphasizing model robustness and reliability, investigating model performance and its standard deviation across folds. Consequently, our study stands as one of the first to extensively validate its findings. To date, the only study that prioritized validation in the ASD assessment domain is the work of Vabalas *et al.* [13], which achieved lower accuracy (73%) and reported greater model variability across folds.

Moreover, the current literature suggests a variety of tasks for ASD assessment using feature-engineered machine learning models. In our work, we concentrated on evaluating the generalizability of these models across various virtual tasks with slightly varying objectives. Alcañiz *et al.* [23] previously employed multiple tasks in a study involving VR, yet they did not utilize these tasks for model comparison or task validation for ASD assessment; their focus was primarily on enhancing classification. Our contribution to the literature lies in the comparison of models trained with every task-specific dataset, resulting in valuable insights such as task validation, model prediction errors, and model reliability based on tasks or how feature-engineered models generalize to different contexts within the same domain. Remarkably, both machine learning and deep learning models concur that, for kinematic data in virtual reality, the most effective task is touching moving objects. However, they diverge when it comes to tasks related to picking up and dropping virtual objects, where feature-engineered models underperform, while end-to-end deep learning models excel.

The final contribution to the existing literature is our deep learning 3DCNN ResNet strategy, which outperforms the

current state-of-the-art in terms of accuracy. The predominant end-to-end deep learning ASD assessment literature is primarily led by Kojovic *et al.* [28] and Zunino *et al.* [27], who reported accuracies of 80.9% and 75%, respectively. Although our ensemble deep learning model attains a slightly lower accuracy than that of Kojovic *et al.* [28], with our model achieving 77% (SD = 10%), our best task-specific deep learning model reaches an accuracy of 85% (SD=3%) with a 1-to-3-minute sample, surpassing their results. It is worth noting that Kojovic *et al.* [28] utilized much longer 1-hour video samples to achieve their reported performance. Notably, Kojovic *et al.* [28] reported that using shorter 10-minute video segments for training reduced their accuracy to approximately 70%, and it dropped even further to around 65% when using 1-to-5-minute samples. In contrast, Zunino *et al.* [27] achieved a lower classification accuracy than our deep learning ensemble model, with a reported accuracy of 75%. The primary distinction between their works and ours lies in the use of 3D kernels to elaborate features based on both time and space, rather than solely space. In their works, Kojovic *et al.* [28] and Zunino *et al.* [27] both extracted spatial features and employed LSTM for temporal classification of the time series. However, our results suggest that enabling time and spatial correlations to emerge improves performance. This approach presumably enables the network to capture spatial and temporal correlations, crucial for movement classification, resulting in enhanced feature engineering, better performance across various contexts, and ultimately, improved generalization and reliability.

7. Conclusion

This study addresses the critical need for more rigorous and dependable ASD assessment methods, while simultaneously conducting a thorough comparison between end-to-end deep learning models and feature-engineered counterparts within a virtual reality environment encompassing diverse motor tasks. Our findings indicate that conventional models can indeed achieve state-of-the-art performance, while also providing benefits towards explainability. However, they exhibit less stability and greater variability across different contextual applications within the domain of the study. In contrast, deep learning approaches not only achieve comparable state-of-the-art performance but also showcase remarkable robustness and generalizability, all without necessitating the expertise required for manual feature engineering. In essence, our research highlights that deep learning methods possess the innate ability to autonomously derive meaningful features from movement data, transcending the constraints of specific task contexts and objectives. This inherent adaptability positions deep learning as a potent and reliable tool for ASD classification, shedding light on the intricate movement patterns associated with the disorder.

References

- [1] American Psychiatric Association. and American Psychiatric Association. *Diagnostic and statistical manual of mental disorders : DSM-5*. American Psychiatric Association Arlington, VA, 5th ed. edition, 2013. ISBN 089042554 0890425558 9780890425541 9780890425558. [1](#)
- [2] Matson JL, Benavidez DA, Compton LS, Paclawskyj T, and Baglio C. Behavioral treatment of autistic persons: a review of research from 1980 to the present. *Res Dev Disabil*. 1996 Nov-Dec;17(6):433-65. doi: 10.1016/j.ridd.2017.10.025. [1](#)
- [3] Anjana Bhat. Motor impairment increases in children with autism spectrum disorder as a function of social communication, cognitive and functional impairment, repetitive behavior severity, and comorbid diagnoses: A spark study report. *Autism Research*, 14, 12 2020. doi:10.1002/aur.2453. [1](#)
- [4] Leo Kanner et al. Autistic disturbances of affective contact. *Nervous child*, 2(3):217–250, 1943. [1](#)
- [5] Martha Leary and D.A. Hill. Moving on: Autism and movement disturbance. *Mental retardation*, 34:39–53, 03 1996.
- [6] Martin McPhillips, Jennifer Finlay, Susanne Berjerot, and Mary Hanley. Motor deficits in children with autism spectrum disorder: A cross-syndrome study. *Autism Research*, 7(6):664–676, 2014. doi:<https://doi.org/10.1002/aur.1408>.
- [7] Maninderjit Kaur, Sudha M. Srinivasan, and Anjana N. Bhat. Comparing motor performance, praxis, coordination, and interpersonal synchrony between children with and without autism spectrum disorder (asd). *Research in Developmental Disabilities*, 72:79–95, 2018. ISSN 0891-4222. doi:<https://doi.org/10.1016/j.ridd.2017.10.025>.
- [8] Yi Lim, Melissa Licari, Alicia Spittle, Rochelle Watkins, Jill Zwicker, Jenny Downs, and Amy Finlay-Jones. Early motor function of children with autism spectrum disorder: A systematic review. *Pediatrics*, 147, 01 2021. doi:10.1542/peds.2020-011270.
- [9] John Stins and Claudia Emck. Balance performance in autism: A brief overview. *Frontiers in Psychology*, 9, 06 2018. doi:10.3389/fpsyg.2018.00901.
- [10] Deborah Dewey, Marja Cantell, and Susan Crawford. Motor and gestural performance in children with autism spectrum disorders, developmental coordination disorder, and/or attention deficit hyperactivity disorder. *Journal of the International Neuropsychological Society : JINS*, 13:246–56, 04 2007. doi:10.1017/S1355617707070270.
- [11] Amanda Fleury, Azadeh Kushki, Nadia Tanel, Evdokia Anagnostou, and Tom Chau. Statistical persistence and timing characteristics of repetitive circle drawing in children with asd. *Developmental Neurorehabilitation*, 16(4):245–254, 2013. doi:10.3109/17518423.2012.758184. PMID: 23477404.
- [12] Alessandro Crippa, Christian Salvatore, Paolo Perego, Sara Forti, Maria Nobile, Molteni Massimo, and Isabella Castiglioni. Use of machine learning to identify children with autism and their motor abnormalities. *Journal of autism and developmental disorders*, 45, 02 2015. doi:10.1007/s10803-015-2379-8. [2](#), [3](#), [5](#), [12](#)
- [13] Andrius Vabalas, Emma Gowen, Ellen Poliakoff, and Alex Casson. Applying machine learning to kinematic and eye movement features of a movement imitation task to predict autism diagnosis. *Scientific Reports*, 10, 05 2020. doi:10.1038/s41598-020-65384-4. [1](#), [2](#), [3](#), [5](#), [12](#)
- [14] Zsanett Péter, Melody Oliphant, and Thomas Fernandez. Motor stereotypies: A pathophysiological review. *Frontiers in Neuroscience*, 11, 03 2017. doi:10.3389/fnins.2017.00171. [1](#)
- [15] Ghanizadeh A. *Clinical approach to motor stereotypies in autistic children*. PMC3446025, Jun;20(2):149-59. PMID: 23056697; PMCID, 2010. [1](#)
- [16] Harris KM, Mahone EM, and Singer HS. Nonautistic motor stereotypies: clinical features and longitudinal follow-up. *Pediatr Neurol*. 2008 Apr;38(4):267-72. doi: 10.1016/j.pediatrneurol.2008.04.006. [1](#)
- [17] Md. Zasim Uddin, Md. Arif Shahriar, Md. Nadim Mahamood, Fady Alnajjar, Md. Ileas Pramanik, and Md Atiqur Rahman Ahad. Deep learning with image-based autism spectrum disorder analysis: A systematic review. *Engineering Applications of Artificial Intelligence*, 127:107185, 2024. ISSN 0952-1976. doi:<https://doi.org/10.1016/j.engappai.2023.107185>. URL <https://www.sciencedirect.com/science/article/pii/S0952197623013696>. [1](#)
- [18] Nuno Bento, Joana Rebelo, Marília Barandas, André V. Carreiro, Andrea Campagner, Federico Cabitza, and Hugo Gamboa. Comparing handcrafted features and deep neural representations for domain generalization in human activity recognition. *Sensors*, 22(19), 2022. ISSN 1424-8220. doi:10.3390/s22197324. URL <https://www.mdpi.com/1424-8220/22/19/7324>. [2](#)
- [19] Anibal Sólón Heinsfeld, Alexandre Rosa Franco, R. Cameron Craddock, Augusto Buchweitz, and Felipe Meneguzzi. Identification of autism spectrum disorder using deep learning and the abide dataset. *NeuroImage: Clinical*, 17:16–23, 2018. ISSN 2213-1582. doi:<https://doi.org/10.1016/j.nicl.2017.08.017>. URL <https://www.sciencedirect.com/science/article/pii/S1552281817322222>. [1](#)

com / science / article / pii / S2213158217302073. 2

- [20] Jundong Li, Kewei Cheng, Suhang Wang, Fred Morstatter, Robert P. Trevino, Jiliang Tang, and Huan Liu. Feature selection: A data perspective. *ACM Computing Surveys*, 50(6):1–45, December 2017. ISSN 1557-7341. doi:[10.1145/3136625](https://doi.org/10.1145/3136625). URL <http://dx.doi.org/10.1145/3136625>. 2
- [21] George Trigeorgis, Fabien Ringeval, Raymond Brueckner, Erik Marchi, Mihalis A. Nicolaou, Björn Schuller, and Stefanos Zafeiriou. Adieu features? end-to-end speech emotion recognition using a deep convolutional recurrent network. In *2016 IEEE International Conference on Acoustics, Speech and Signal Processing (ICASSP)*, pages 5200–5204, 2016. doi:[10.1109/ICASSP.2016.7472669](https://doi.org/10.1109/ICASSP.2016.7472669). 2
- [22] Sara Forti, Angela Valli, Paolo Perego, Maria Nobile, Alessandro Crippa, and Molteni Massimo. Motor planning and control in autism. a kinematic analysis of preschool children. *Research in Autism Spectrum Disorders*, 5:834–842, 04 2011. doi:[10.1016/j.rasd.2010.09.013](https://doi.org/10.1016/j.rasd.2010.09.013). 2, 5
- [23] Mariano Alcañiz Raya, Javier Marín-Morales, Maria Eleonora Minissi, Gonzalo Teruel García, Luis Abad, and Irene Chicchi Giglioli. Machine learning and virtual reality on body movements’ behaviors to classify children with autism spectrum disorder. *Journal of Clinical Medicine*, 9:1260, 04 2020. doi:[10.3390/jcm9051260](https://doi.org/10.3390/jcm9051260). 3, 12
- [24] Roberta Simeoli, Nicola Milano, Angelo Rega, and Davide Marocco. Using technology to identify children with autism through motor abnormalities. *Frontiers in Psychology*, 12:635696, 05 2021. doi:[10.3389/fpsyg.2021.635696](https://doi.org/10.3389/fpsyg.2021.635696).
- [25] Zhong Zhao, Haiming Tang, Camila Alviar, Christopher Kello, Xiaobin Zhang, Xinyao hu, Xingda Qu, and Jianping Lu. Excessive and less complex body movement in children with autism during face-to-face conversation: An objective approach to behavioral quantification. *Autism Research*, 15, 11 2021. doi:[10.1002/aur.2646](https://doi.org/10.1002/aur.2646). 2, 3, 5, 12
- [26] Simeoli R, Milano N, Rega A, and Marocco D. Using technology to identify children with autism through motor abnormalities. *Front Psychol*. 2021 May 25;12:635696. doi: [10.3389/fpsyg.2021.635696](https://doi.org/10.3389/fpsyg.2021.635696). 10., 2021. 2, 3, 12
- [27] Andrea Zunino, Pietro Morerio, Andrea Cavallo, Caterina Ansuini, Jessica Podda, Francesca Battaglia, Edvige Veneselli, Cristina Becchio, and Vittorio Murino. Video gesture analysis for autism spectrum disorder detection. In *2018 24th International Conference on Pattern Recognition (ICPR)*, pages 3421–3426, 2018. doi:[10.1109/ICPR.2018.8545095](https://doi.org/10.1109/ICPR.2018.8545095). 3, 12
- [28] Nada Kojovic, Shreyasvi Natraj, Sharada Mohanty, Thomas Maillart, and Marie Schaer. Using 2d video-based pose estimation for automated prediction of autism spectrum disorders in young children. *Scientific Reports*, 11:15069, 07 2021. doi:[10.1038/s41598-021-94378-z](https://doi.org/10.1038/s41598-021-94378-z). 3, 12
- [29] Biomarkers Definitions Working Group.. Biomarkers and surrogate endpoints: preferred definitions and conceptual framework. *Clin Pharmacol Ther*. 2001 Mar;69(3):89-95. doi: [10.1016/S0009-2502\(00\)01611-1](https://doi.org/10.1016/S0009-2502(00)01611-1). 10., 2001. 3
- [30] Lord C, Risi S, Lambrecht L, Cook EH Jr, Leventhal BL, DiLavore PC, Pickles A, and Rutter M. The autism diagnostic observation schedule-generic: a standard measure of social and communication deficits associated with the spectrum of autism. *J Autism Dev Disord*. 2000 Jun;30(3):205-23. PMID: [11055457](https://pubmed.ncbi.nlm.nih.gov/11055457/)., 2000. 3
- [31] Maria Eleonora MINISSI, Irene Alice CHICCHI GIGLIOLI, Fabrizia MANTOVANI, Marian SIRERA, Luis ABAD, and Mariano ALCANIZ. A qualitative and quantitative virtual reality usability study for the early assessment of asd children. *ANNUAL REVIEW OF CYBERTHERAPY AND TELEMEDICINE 2021*, page 47, 2021. 3
- [32] Emiliano Pastorelli and Heiko Herrmann. A small-scale, low-budget semi-immersive virtual environment for scientific visualization and research. *Procedia Computer Science*, 25:14–22, 2013. 3
- [33] Simon Wallace, Sarah Parsons, Alice Westbury, Katie White, Kathy White, and Anthony Bailey. Sense of presence and atypical social judgments in immersive virtual environments responses of adolescents with autism spectrum disorders. *Autism : the international journal of research and practice*, 14:199–213, 05 2010. doi:[10.1177/1362361310363283](https://doi.org/10.1177/1362361310363283).
- [34] Sarah Sharples, Sue Cobb, Amanda Moody, and John Wilson. Virtual reality induced symptoms and effects (vrise): Comparison of head mounted display (hmd), desktop and projection display systems. *Displays*, 29: 58 – 69, 03 2008. doi:[10.1016/j.displa.2007.09.005](https://doi.org/10.1016/j.displa.2007.09.005). 3
- [35] Haodong Duan, Yue Zhao, Kai Chen, Dahua Lin, and Bo Dai. Revisiting skeleton-based action recognition, 2022. 7